AJNR

Asynchrony in Peritumoral Resting-State Blood Oxygen Level–Dependent fMRI Predicts Meningioma Grade and Invasion

P.B. Wu, D.S. Chow, P.D. Petridis, M.B. Sisti, J.N. Bruce, P.D. Canoll and J. Grinband

Asynchrony in Peritumoral Resting-State Blood Oxygen Level–Dependent fMRI Predicts Meningioma Grade and Invasion

P.B. Wu, D.S. Chow, P.D. Petridis, M.B. Sisti, J.N. Bruce, P.D. Canoll, and J. Grinband

ABSTRACT

BACKGROUND AND PURPOSE: Meningioma grade is determined by histologic analysis, with detectable brain invasion resulting in a diagnosis of grade II or III tumor. However, tissue undersampling is a common problem, and invasive parts of the tumor can be missed, resulting in the incorrect assignment of a lower grade. Radiographic biomarkers may be able to improve the diagnosis of grade and identify targets for biopsy. Prior work in patients with gliomas has shown that the resting-state blood oxygen level–dependent fMRI signal within these tumors is not synchronous with normal brain. We hypothesized that blood oxygen level–dependent asynchrony, a functional marker of vascular dysregulation, could predict meningioma grade.

MATERIALS AND METHODS: We identified 25 patients with grade I and 11 patients with grade II or III meningiomas. Blood oxygen level–dependent time-series were extracted from the tumor and the radiographically normal control hemisphere and were included as predictors in a multiple linear regression to generate a blood oxygen level–dependent asynchrony map, in which negative values signify synchronous and positive values signify asynchronous activity relative to healthy brain. Masks of blood oxygen level–dependent asynchrony were created for each patient, and the fraction of the mask that extended beyond the contrast-enhancing tumor was computed.

RESULTS: The spatial extent of blood oxygen level–dependent asynchrony was greater in high (grades II and III) than in low (I) grade tumors ($P < 0.001$) and could discriminate grade with high accuracy (area under the curve = 0.88).

CONCLUSIONS: Blood oxygen level–dependent asynchrony radiographically discriminates meningioma grade and may provide targets for biopsy collection to aid in histologic diagnosis.

ABBREVIATIONS: AUC = area under the curve; BOF = BOLD outside fraction; BOLD = blood oxygen level–dependent; FOF = FLAIR outside fraction

The 2016 World Health Organization guidelines for meningiomas were notable for the inclusion of brain invasion as a criterion sufficient for assignment to "high-grade" status (ie, grade II or III) and may explain the greater incidence of high-grade meningiomas since 2016.[1] In addition to brain invasion, a meningioma is considered grade II or III if it demonstrates an elevated mitotic index and ≥3 aggressive histologic features or demonstrates a loss of meningothelial differentiation.[2] While roughly 80% of all meningiomas are grade I, with excellent prognosis

following surgical resection, the remaining 20% are grade II or III and more likely to recur.[3] Furthermore, grade I tumors have a 10-year survival of 83%, compared with 61% for grade II and III tumors,[4] making the accurate determination of meningioma grade important for both prognostic and treatment purposes.

Histologic assessment remains the criterion standard for grading meningiomas; however, an accurate noninvasive prediction of tumor grade could benefit both clinicians and patients by improving preoperative planning and patient counseling and potentially guiding difficult management decisions. Furthermore, routine surgical biopsy may undersample regions that have histologic features, such as invasion, that are diagnostic for grade II or III meningioma, resulting in possible misdiagnosis. Identifying radiographic features that correlate with tumor invasion would, therefore, be useful for guiding biopsy location. Prior studies using standard-of-care structural imaging have attempted to predict meningioma grade by evaluating a mix of objective radiographic features, such as mean voxel intensity, and subjective radiographic features, such as the presence of hyperostosis.[5] Peritumoral edema detected by T2-FLAIR has also

been associated with higher-grade meningiomas.[6,7] Additionally, histogram analysis of diffusion tensor imaging has also been shown to correlate with tumor grade and tumor subtype in meningiomas.[8] However, it would be beneficial to develop a single, simple, visual criterion that could be easily applied by radiologists and surgeons to predict meningioma grade with high accuracy.

Prior work using resting-state blood oxygen level—dependent (BOLD) fMRI in diffuse glioma has revealed that the BOLD signal in and around the tumor is temporally asynchronous with radiographically normal parts of the brain.[9] BOLD asynchrony maps provide a quantitation of this phenomenon and are generated by comparing each voxel with the mean global signal intensity of both the contralesional hemisphere and the contrast-enhancing tumor. Stereotactically localized biopsies collected from peritumoral regions have demonstrated that the degree of BOLD asynchrony correlates with local tumor burden.[10] Furthermore, the spatial extent of the asynchrony can discriminate *IDH* wild-type and *IDH*-mutated gliomas with high fidelity.[11]

Meningiomas have also been shown to cause disruptions in vascular function observable with resting-state BOLD fMRI.[11] We, therefore, hypothesized that brain invasion, a common feature of high-grade meningiomas, would be detectable using BOLD asynchrony maps derived from resting-state BOLD fMRI and that the spatial extent of BOLD asynchrony could be used to discriminate meningioma grade. Furthermore, we evaluated whether combining the spatial features of BOLD asynchrony and T2-FLAIR hyperintensity could improve tumor grading accuracy over either measure alone.

MATERIALS AND METHODS
Patient Selection and Clinical Data Acquisition
All aspects of this single-center study were conducted in compliance with the Health Insurance Portability and Accountability Act regulations and approved by the institutional review board of Columbia University. Demographic and clinical data were retrospectively collected from the medical records of patients diagnosed with meningiomas and treated at our institution between 2010 and 2020. Pathology reports generated before the release of the 2016 World Health Organization criteria were re-evaluated to ensure that all tumors were graded correctly according to the updated 2016 criteria. Patients were included in the study if they were at least 18 years of age, had histologically proved meningiomas, and had preoperative structural MR imaging and resting-state BOLD fMRI available. The reported patient age was dated from the time the BOLD fMRI scan was acquired. Because our cohort included only a single patient with grade III, this patient was grouped with grade II patients into a "high-grade" meningioma group. All patients had preoperative standard-of-care T1 postcontrast and T2-FLAIR sequences, in addition to resting-state BOLD fMRI. Imaging parameters are listed in the Online Supplemental Data. Contrast-enhanced images were obtained with intravenous gadobenate dimeglumine (MultiHance; Bracco Diagnostics) dosed by weight at 0.2 mL/kg. BOLD images were obtained before contrast administration.

Structural ROIs
Tumor masks were defined by contrast enhancement on T1-weighted imaging and were hand-drawn by a board-certified neuroradiologist with 10 years of experience (D.S.C.) as described previously in Chow et al.[9] In this study, normal brain comprised the cerebral hemisphere contralateral to the tumor with any contrast enhancement or T2-FLAIR hyperintensity crossing the midline removed. Masks of peritumoral edema were also drawn from each patient's corresponding T2-FLAIR imaging after being affine-registered with 6 *df* to their corresponding T1-postcontrast image using the FMRIB Linear Image Registration Tool, Version 5.0.6 (FLIRT; http://www.fmrib.ox.ac.uk/fslwiki/FLIRT).[12] Registrations were visually inspected to ensure high-quality alignment. All masks were drawn in a blinded manner with the neuroradiologist unaware of the histologic subtype of the tumor or the radiographic features present on other sequences.

BOLD Asynchrony Maps
Overview. Global signal intensity refers to the mean BOLD signal across the entire brain and is related to cardiac pulsations and respiration-related changes in arterial carbon dioxide (CO_2)[12-14] as well as whole-brain neural fluctuations.[15] Vascular sources account for ~25%–27% of the variance, and neural sources account for ~5%–6% of the variance in the global signal.[16,17] Also, by means of functional connectivity measures, the 2 hemispheres are >95% symmetric.[18] This signal is often considered a nuisance variable that is removed as part of standard BOLD preprocessing.[19,20] In the current study, the global signal of the control mask is used as a temporal signature of healthy hemodynamics reflecting normal responses to cardiac pulsatility, respiration-related CO_2 changes, and neuronal fluctuations common across the whole brain. The mean signal from the tumor mask produces a temporal signature of unhealthy hemodynamics. Voxelwise regression using these 2 signatures produces 2 Z-statistic maps that represent the similarity of each voxel to tumor and normal brain. Furthermore, because the tumor and control time-series are temporally uncorrelated, subtracting the 2 maps further enhances the difference between the 2 tissue types and results in a map of BOLD asynchrony.[9] The degree of asynchrony has been shown to predict tumor burden, thus providing an indirect measure of glioma brain invasion.[10]

Preprocessing. Resting-state BOLD fMRI data were preprocessed as previously described.[9] Briefly, the imaging data were brain-extracted, motion-corrected, slice timing–corrected, spatially smoothed (Gaussian filter, full width at half maximum = 5 mm), high-pass-filtered, and coregistered (linear, 6 *df*) to the T1-postcontrast image using FSL (http://www.fmrib.ox.ac.uk/fsl).[21] Independent-components analysis (MELODIC-FIX; https://fsl.fmrib.ox.ac.uk/fsl/fslwiki/MELODIC; https://fsl.fmrib.ox.ac.uk/fsl/fslwiki/FIX) was used to remove artifacts due to scanner noise and head motion.

Mask Generation. Multiple linear regression was performed on each subject's native resting-state BOLD data using time-series extracted from the contrast-enhancing tumor mask and control hemisphere mask. The model also included 6 motion confound

regressors (3 translations and 3 rotations). Two Z-statistic images were then generated, indicating the similarity of each voxel's dynamics to the dynamics of the contrast-enhancing mask and the control hemisphere mask. Because the time-series from the 2 masks are uncorrelated, they can be combined to improve the signal-to-noise properties of the BOLD asynchrony metric.[9] Thus, BOLD asynchrony was defined as the difference of the 2 Z-statistic images ($z_{tumor} - z_{control}$) so that values are negative (blue) in normal brain and positive (red) in regions of tumor-related vascular dysregulation. Moreover, a positive BOLD asynchrony value in a voxel denotes BOLD dynamics that are asynchronous with normal cardiovascular fluctuations. BOLD asynchrony maps were thresholded at $Z > 1.68$ (corresponding to a P value $< .05$ on a standardized normal distribution) to denote voxels with abnormal values, as described previously.[9]

Spatial Decay

To compute the spatial rate of change in the BOLD asynchrony and T2-FLAIR images, we extracted all voxels within a 3-cm radius of the contrast-enhancing tumor and contained within the skull and fit them to an exponential decay of the form

$$N(t) = N_0 e^{-\lambda t},$$

where N represents BOLD asynchrony or T2-FLAIR values.

BOLD and FLAIR Outside Fraction

The BOLD outside fraction (BOF) represents how much of the BOLD asynchronous region is found outside the contrast-enhancing tumor and is calculated by dividing the volume of the BOLD asynchrony mask that extends outside the region of contrast enhancement by the total volume of the BOLD asynchrony mask,

$$BOF = \frac{|BOLD \notin TUMOR|}{|BOLD|}.$$

FLAIR outside fraction (FOF) was computed in a similar way, denoting the fraction of T2-FLAIR hyperintensity outside the contrast-enhancing tumor.

Statistical Analysis

All statistical tests were performed in Matlab 2019a (MathWorks) and thresholded for significance at $P < .05$. The Pearson correlation was calculated using a linear model. Two-tailed Student t tests were used for all paired comparisons. All proportion data were first transformed using the arcsine transform for fractions.

RESULTS

Patient Demographics

We identified 36 patients who underwent standard-of-care imaging with additional resting-state BOLD fMRI before a histologic tumor diagnosis of meningioma. Of these patients, 25 (69%) were diagnosed with grade I meningioma and 11 (31%) were diagnosed with grade II or III meningioma. For this study, the grade II and III meningiomas were grouped together as "high-grade" meningiomas, while grade I tumors were considered "low-grade." The median age of the patients with low-grade tumors was 67 years (range, 29–85 years), and 72%
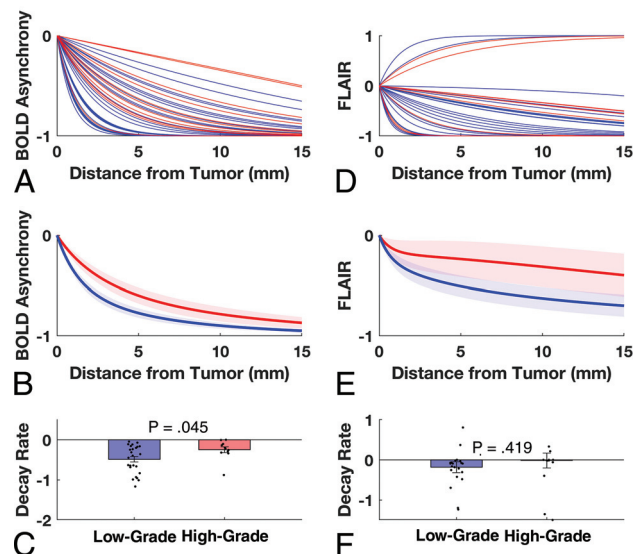

FIG 1. BOLD asynchrony decreases with distance from the tumor. *A,* Exponential fits were made to BOLD asynchrony values across all voxels within a 3-cm radius as a function of distance from the tumor for each patient. *Blue lines* represent individual patients with low-grade tumors; *red lines* represent individual patients with high-grade tumors. *B,* The mean BOLD asynchrony is greater for high-grade than low-grade tumors at comparable distances from the tumor. *Shading* represents standard error of the mean. *C,* Bars represent the median spatial decay for the low- (blue) and high-grade (red) tumors; *dots* represent decay constants for individual patients. High-grade meningiomas have significantly slower spatial decay rates, indicating that high-grade tumors caused a larger disruption to surrounding vasculature. *D–F,* FLAIR signal did not differ significantly between groups. Note, the *error bars* are very large and extend beyond the visible range.

were women; the median age of patients with high-grade tumors was 59 years (range, 41–78 years), and 45% were women.

Spatial Decay of BOLD Asynchrony Differs between Low- and High-Grade Meningiomas

We first tested whether there were objective differences in the spatial extent of BOLD asynchrony between low- and high-grade meningiomas. Tumor-related disruption of vascular function in surrounding tissue should result in higher BOLD asynchrony values. To this end, we plotted the BOLD asynchrony signal in each voxel as a function of distance from contrast-enhancing tumor or all brain voxels in a 3-cm radius around the tumor. BOLD asynchrony decreased as a function of distance for all patients (Fig 1A) but decreased faster in low-grade tumors (Fig 1B). A comparison of decay rates showed a significant difference between the 2 groups, with high-grade meningiomas showing a smaller rate (ie, slower spatial decay) than low-grade tumors (high-grade: −0.25; low-grade: −0.49; t test, $P = .045$) (Fig 1C). The T2 FLAIR signal also showed a slower decay in high-grade tumors, though this difference was not significant (high-grade: −0.25; low-grade: −0.45; t test, $P = .42$) (Fig 1D–F).

Extent of BOLD Asynchrony and T2-FLAIR Hyperintensity Discriminate Meningioma Grade

Although the spatial-decay analysis is objective, an arbitrary 3-cm margin is likely to include voxels affected and unaffected by
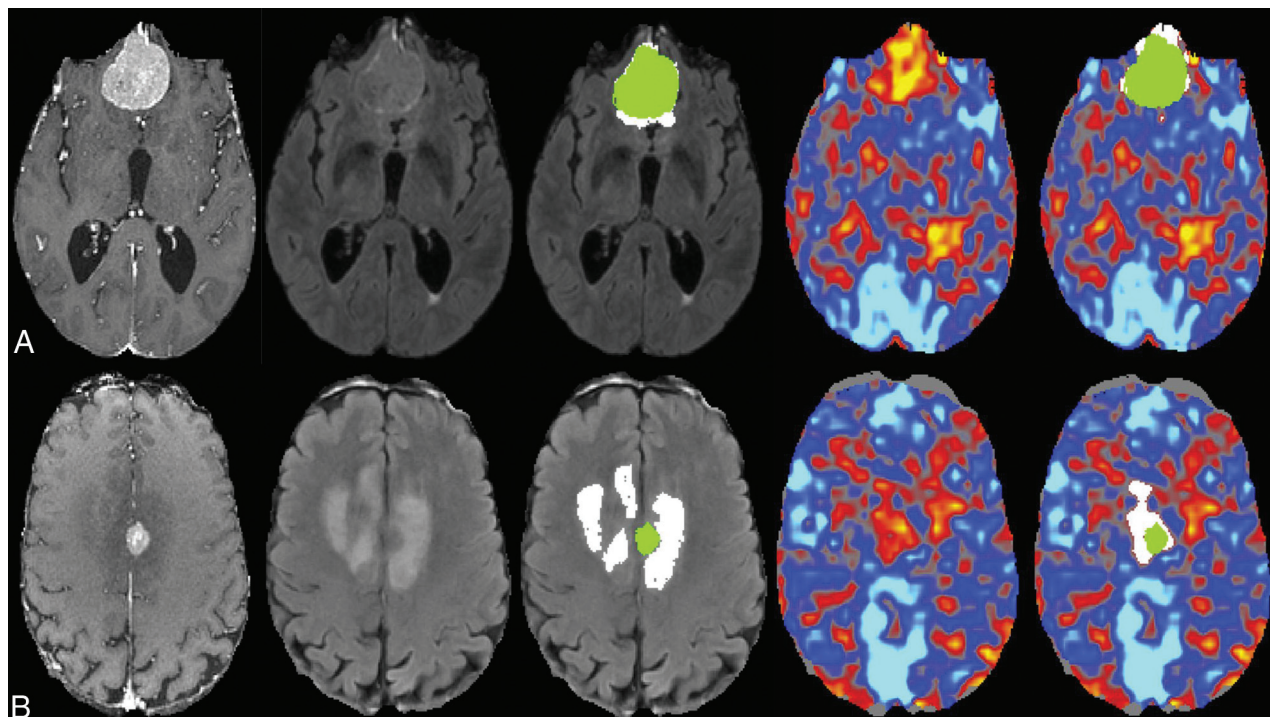
FIG 2. Representative axial slices from a 77-year-old male patient (*A*) with a grade I meningioma and a 75-year-old male patient (*B*) with a grade II meningioma. The first 3 columns show the T1-weighted postcontrast image, the T2-FLAIR, and the T2-FLAIR with overlaid masks representing the contrast enhancement (green) and the T2-FLAIR hyperintensity outside the tumor (white). The fourth and fifth columns show the BOLD asynchrony map and the BOLD asynchrony map with overlaid masks representing the contrast enhancement (green) and the BOLD asynchrony outside the tumor (white). The high-grade tumor (*B*) has BOLD asynchrony extending further outside the region of contrast enhancement than the low-grade tumor.

tumor, resulting in a mixture of low and high decay rates, which may underestimate differences between groups. To address this issue, we used subjective, expert-drawn masks of the elevated BOLD asynchrony to estimate the size of the tumor-related increases in BOLD asynchrony and determine whether it differed across grades. Sample T1-weighted postcontrast, T2-FLAIR, and BOLD asynchrony images from patients with grade I and II tumors are shown in Fig 2. The BOF and FOF are greater in the high-grade tumor than in the low-grade tumor.

The mean BOF across subjects was significantly greater in the high-grade than the low-grade meningiomas (high-grade: 0.33; low-grade: 0.17; *t* test, *P* < .001) (Fig 3*A*). We also found that the mean FOF was higher in the high-grade tumors (0.43 versus 0.23, *P* = .092), though this did not reach significance (Fig 3*B*). A receiver-operating characteristic curve was generated for the BOF (Fig 3*C*) and FOF (Fig 3*D*) to assess how well these 2 measures can discriminate between the 2 groups. The area under the curve (AUC) for the BOF was 0.88, while for FOF, it was 0.67. Sample cases in which BOF and FOF were discordant in their tumor-grade prediction are shown in the Online Supplemental Data.

Combining Structural and Functional Imaging Improves Discrimination
BOLD asynchrony and T2-FLAIR hyperintensity discriminate meningioma grade through fundamentally different processes, ie,

vascular function versus edema, and in fact, the 2 measures were not significantly correlated (*r* = 0.12, *P* = .50). This finding suggests that combining the 2 measures could improve discriminability over either measure alone. A weighted mean fit showed that the best model (0.86 × BOF + 0.14 × FOF) resulted in a modest improvement in discriminability (high-grade mean: 0.34; low-grade mean: 0.18; *t* test, *P* < .001) (Fig 4*A*) with an area under the curve of 0.90 (Fig 4*B*).

DISCUSSION
Accurate preoperative prediction of tumor grade enhances patient counseling and may inform clinical decision-making regarding treatment of patients when there is clinical equipoise. For instance, a suspected high-grade meningioma may merit more aggressive treatment than a suspected low-grade meningioma and advanced knowledge that a tumor shows brain invasion might alter the surgical approach. Furthermore, current pathologic diagnosis of brain invasion is limited by sampling error. A radiographic biomarker of brain invasion could greatly increase the likelihood of successfully sampling invasive tissue and correctly grading the tumor.

In this study, we looked at the patterns of BOLD asynchrony and T2-FLAIR hyperintensity in grade I, II, and III meningiomas. The spatial decay rate of BOLD asynchrony was significantly different in low- and high-grade meningiomas. Furthermore, because brain invasion is often focal and not uniformly distributed, we used expert-drawn masks to
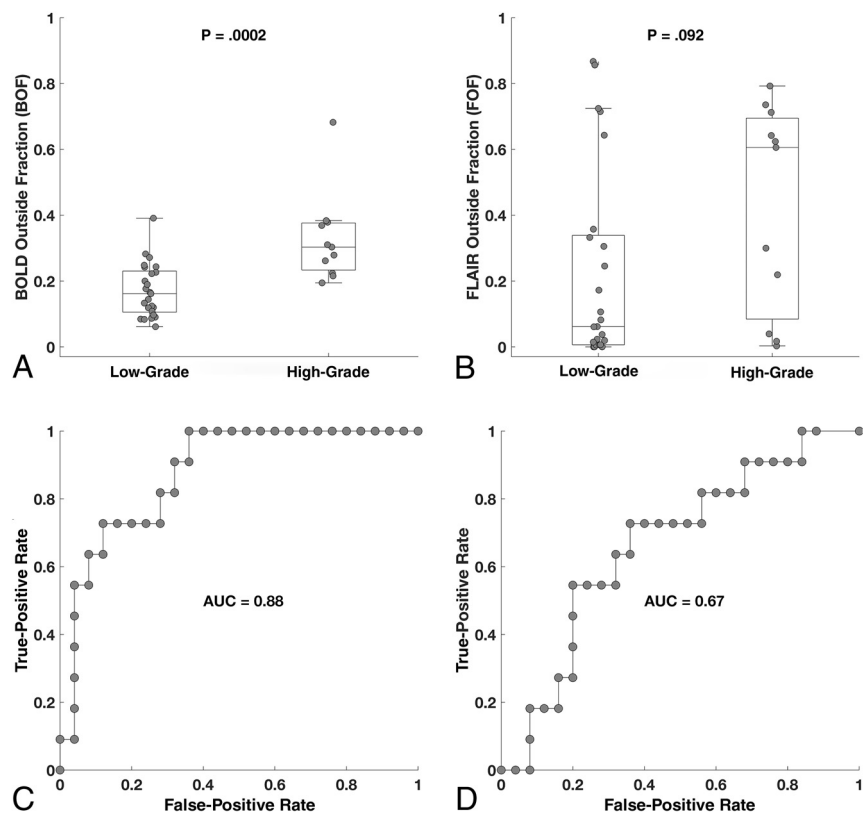
FIG 3. Boxplots demonstrate that high-grade meningiomas are characterized by greater BOF values than low-grade meningiomas (*A*). *B*, FOF values were higher in high-grade meningiomas, though this did not reach significance. Receiver operating characteristic curves for BOF show high discriminability for grade (*C*), while FOF demonstrates marginal discriminability (*D*).
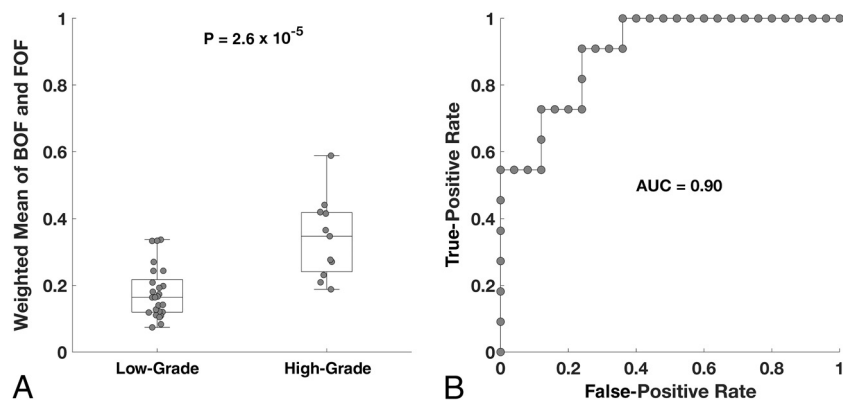

FIG 4. *A*, The weighted mean of BOF and FOF shows a difference comparable with the BOF alone. *B*, The discriminability of the weighted model is better, though only marginally, than the BOF alone.

measure the extent of BOLD asynchrony outside the contrast-enhancing tumor (BOF) and found even better discriminability between low- and high-grade meningiomas. Previous work[6,7] has suggested that peritumoral edema is associated with high-grade meningiomas; however, in our sample, the FOF was not significantly different between the 2 tumor groups.

BOF and FOF have areas under the curve of 0.88 and 0.67, respectively, suggesting that BOLD asynchrony is superior to T2-FLAIR hyperintensity for discriminating tumor grade. When combining the 2, the area under the curve improves slightly to 0.90. This outcome is consistent with our understanding that T2-FLAIR and BOLD asynchrony measure independent physiologic processes—edema for T2-FLAIR hyperintensity and abnormal vascular function for BOLD asynchrony. This discrimination accuracy is comparable with previously published values of AUC = 0.946 for DTI histogram analysis and AUC = 0.86 for multiple standard-of-care imaging features.[5,8] Although generating a weighted mean estimate would likely be impractical for a typical clinician, visual inspection of the T2-FLAIR and BOLD asynchrony maps may allow a fast and accurate determination of tumor grade by a trained neuroradiologist or neurosurgeon. Prospective application of this methodology for predicting grade will be needed to determine its true efficacy, accessibility, and value to clinicians.

Prior work in glioma has shown that BOLD asynchrony correlates with tumor burden in gliomas, suggesting that the presence of local tumor cells causes vascular dysregulation.[10] However, all patients with grade I meningiomas in our cohort had a BOF greater than 0, despite having no evidence of histologic brain invasion. Although the lack of detectable invasion may be at least partly due to tissue-sampling error, the positive BOFs suggest that BOLD asynchrony outside of the region of contrast enhancement is not solely caused by local tumor burden but also by other physiologic mechanisms such as the compression of peritumoral small vessels, compression of large vessels that supply peritumoral small vessels, or compression of local neurons that lead to vascular dysregulation.

One limitation of this study is its retrospective nature and relatively small sample size, which prevented the use of a subset of patients as an independent validation set. Furthermore, due to their rarity, grade III meningiomas could not be analyzed separately from grade II tumors; thus, it is unknown whether BOLD asynchrony can differentiate grade II and III tumors. Finally, future studies using MR imaging–

localized biopsies will be necessary to assess how accurately BOLD asynchrony can predict local tumor burden and whether it can be used as a tool for identifying the locations of putative invasion.

CONCLUSIONS

This study provides preliminary evidence that BOLD asynchrony maps are a useful adjunct for discriminating grade and brain invasion in meningiomas through both the spatial decay rate and BOF.

REFERENCES

1. Kshettry VR, Ostrom QT, Kruchko C, et al. **Descriptive epidemiology of World Health Organization grades II and III intracranial meningiomas in the United States.** *Neuro Oncol* 2015;17:1166–73 CrossRef Medline

2. Louis DN, Perry A, Reifenberger G, et al. **The 2016 World Health Organization Classification of Tumors of the Central Nervous System: a summary.** *Acta Neuropathol* 2016;131:803–20 CrossRef Medline

3. Willis J, Smith C, Ironside JW, et al. **The accuracy of meningioma grading: a 10-year retrospective audit.** *Neuropathol Appl Neurobiol* 2005;31:141–49 CrossRef Medline

4. Ostrom QT, Cioffi G, Gittleman H, et al. **CBTRUS Statistical Report: Primary Brain and Other Central Nervous System Tumors Diagnosed in the United States in 2012-2016.** *Neuro Oncol* 2019;21: v1–100 CrossRef Medline

5. Coroller TP, Bi WL, Huynh E, et al. **Radiographic prediction of meningioma grade by semantic and radiomic features.** *PLoS One* 2017;12:e0187908 CrossRef Medline

6. Kim BW, Kim MS, Kim SW, et al. **Peritumoral brain edema in meningiomas: correlation of radiologic and pathologic features.** *J Korean Neurosurg Soc* 2011;49:26–30 CrossRef Medline

7. Adeli A, Hess K, Mawrin C, et al. **Prediction of brain invasion in patients with meningiomas using preoperative magnetic resonance imaging.** *Oncotarget* 2018;9:35974–82 CrossRef Medline

8. Wang S, Kim S, Zhang Y, et al. **Determination of grade and subtype of meningiomas by using histogram analysis of diffusion-tensor imaging metrics.** *Radiology* 2012;262:584–92 CrossRef Medline

9. Chow DS, Horenstein CI, Canoll P, et al. **Glioblastoma induces vascular dysregulation in nonenhancing peritumoral regions in humans.** *AJR Am J Roentgenol* 2016;206:1073–81 CrossRef Medline

10. Bowden SG, Gill BJ, Englander ZK, et al. **Local glioma cells are associated with vascular dysregulation.** *AJNR Am J Neuroradiol* 2018;39:507–14 CrossRef Medline

11. Jiang Z, Krainik A, David O, et al. **Impaired fMRI activation in patients with primary brain tumors.** *Neuroimage* 2010;52:538–48 CrossRef Medline

12. Murphy K, Birn RM, Handwerker DA, et al. **The impact of global signal regression on resting state correlations: are anti-correlated networks introduced?** *Neuroimage* 2009;44:893–905 CrossRef Medline

13. Shmueli K, van Gelderen P, de Zwart JA, et al. **Low-frequency fluctuations in the cardiac rate as a source of variance in the resting-state fMRI BOLD signal.** *Neuroimage* 2007;38:306–20 CrossRef Medline

14. Birn RM, Murphy K, Bandettini PA. **The effect of respiration variations on independent component analysis results of resting state functional connectivity.** *Hum Brain Mapp* 2008;29:740–50 CrossRef Medline

15. Scholvinck ML, Maier A, Ye FQ, et al. **Neural basis of global resting-state fMRI activity.** *Proc Natl Acad Sci U S A* 2010;107:10238–43 CrossRef Medline

16. Power JD, Plitt M, Laumann TO, et al. **Sources and implications of whole-brain fMRI signals in humans.** *Neuroimage* 2017;146:609–25 CrossRef Medline

17. Glasser MF, Coalson TS, Bijsterbosch JD, et al. **Using temporal ICA to selectively remove global noise while preserving global signal in functional MRI data.** *Neuroimage* 2018;181:692–717 CrossRef Medline

18. Raemaekers M, Schellekens W, Petridou N, et al. **Knowing left from right: asymmetric functional connectivity during resting state.** *Brain Struct Funct* 2018;223:1909–22 CrossRef Medline

19. Murphy K, Birn RM, Bandettini PA. **Resting-state fMRI confounds and cleanup.** *Neuroimage* 2013;80:349–59 CrossRef Medline

20. Desjardins AE, Kiehl KA, Liddle PF. **Removal of confounding effects of global signal in functional MRI analyses.** *Neuroimage* 2001;13:751–58 CrossRef Medline

21. Jenkinson M, Beckmann CF, Behrens TE, et al. **FSL.** *Neuroimage* 2012;62:782–90 CrossRef Medline